

# INTRIGUING INVARIANTS OF CENTERS OF ELLIPSE-INScribed TRIANGLES

MARK HELMAN, RONALDO GARCIA, AND DAN REZNIK\*

**ABSTRACT.** We describe intriguing properties of a 1d family of triangles: two vertices are pinned to the boundary of an ellipse while a third one sweeps it. We prove that: (i) if a triangle center is a fixed affine combination of barycenter and orthocenter, its locus is an ellipse; (ii) over the family of said affine combinations, the centers of said loci sweep a line; (iii) over the family of parallel fixed vertices, said loci rigidly translate along a second line. Additionally, we study invariants of the envelope of elliptic loci over combinations of two fixed vertices on the ellipse.

**Keywords** Ellipse, Locus, Invariant, Envelope, Limaçon.

**MSC** 53A04 and 51M04 and 51N20

## 1. INTRODUCTION

Consider the 1d family of triangles  $\mathcal{T}(t) = V_1V_2P(t)$  where two vertices  $V_1, V_2$  are fixed to the boundary of an ellipse while a third one  $P(t)$  sweeps it. A known property [4] is that over this family, the locus of classic centers such as the bary-, circum-, and orthocenter (denoted  $X_k, k = 2, 3, 4$ , after [13]) are all ellipses; see Figure 1. We further generalize these results and show that:

- If a triangle center  $X_k$  is a fixed affine combination of bary-  $X_2$  and orthocenter  $X_4$ , its locus is an ellipse (co-discovered with A. Akopyan [1]).
- Over the family of said affine combinations, centers of said loci sweep a first line.
- Over parallel  $V_1V_2$ , the elliptic locus of  $X_k$  is a family of ellipses which rigidly translate along a second line passing through  $O$ , the center of  $\mathcal{E}$ .

Additionally, we study the family of elliptic loci of  $X_k$  for fixed  $V_1$  and over all  $V_2$  on  $\mathcal{E}$ . We show that (i) the locus of their centers is an ellipse axis-aligned with  $\mathcal{E}$ , and that (ii) the external envelope to the locus family is invariant over  $V_1$ . In particular, the external envelope of  $X_4$  (resp.  $X_2$ 's) loci is an affine image of Pascal's Limaçon (a 1/3-sized copy of  $\mathcal{E}$ ).

**Related Work.** In [18], an explicit derivation is given for the elliptic locus of the orthocenter for the same triangle family studied in this article. Dykstra et al. [4] derived equations for loci of triangle centers under triangle families with two vertices affixed to special points of the ellipse, including the foci. Loci of triangle centers have been studied for alternative triangle families including: (i)

---

*Date:* September, 2020.

M. Helman, Dept. of Mathematics, Rice University, Houston, TX. [markhelman@hotmail.com](mailto:markhelman@hotmail.com).

R. Garcia, Math. & Stats. Inst., Federal Univ. of Goiás, Goiânia, Brazil. [ragarcia@ufg.br](mailto:ragarcia@ufg.br).

D. Reznik\*, Data Science Consulting Ltd., Rio de Janeiro, Brazil. [dreznik@gmail.com](mailto:dreznik@gmail.com).

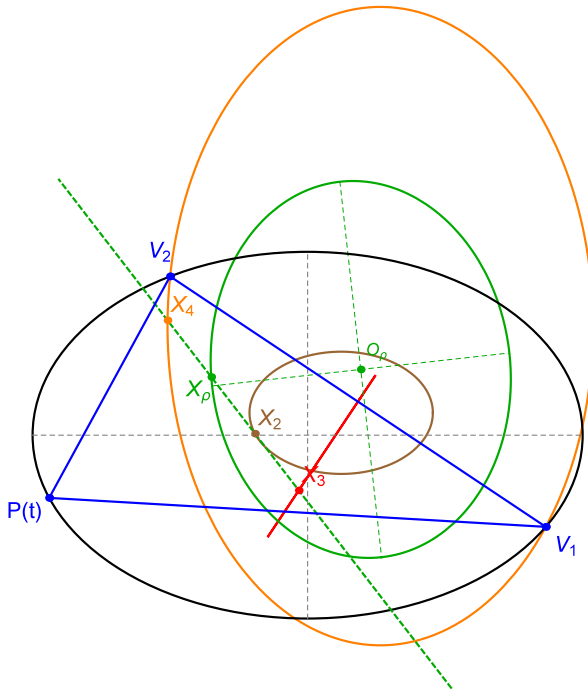


FIGURE 1. A triangle  $V_1V_2P(t)$  (blue) is inscribed in an ellipse  $\mathcal{E}$  (black) with semi-axes  $a, b$ . While  $V_1, V_2$  are fixed,  $P(t)$  executes one revolution along the boundary. Consider triangle centers  $X_k, k = 2, 3, 4$  on the Euler line  $\mathcal{L}_e$  (dashed green). For any choice of  $V_1V_2$ , the locus of (i)  $X_2$  is an axis-aligned ellipse (brown) with semi-axes  $a/3, b/3$ ; (ii)  $X_3$  is a segment (red) contained in the perp. bisector of  $V_1V_2$ ; (iii)  $X_4$  is an axis-aligned ellipse passing through  $V_1, V_2$ , with aspect ratio  $b/a$ . An intermediate point  $X_\rho$  ( $\rho = 1/2$ ) is shown on  $\mathcal{L}_e$  as well as its elliptic locus (green) centered on  $O_\rho$ . Though an ellipse for any  $\rho$ , this locus is in general neither axis-aligned (notice its slanted axes, dashed green), nor similar to  $\mathcal{E}$ . [Video](#)

Poristic triangles (those with fixed incircle and circumcircle) [6, 30, 31, 20]. Odehnal describes pointwise, circular, and elliptic loci for dozens of triangle centers in the poristic family [21]. The poristic family is related via a similarity transform to another “famous” family: 3-periodics in the elliptic billiard [9]; (ii) triangles with common incircle and centroid. Pamfilos has shown their vertices lie on a conic [22]; (iii) Triangles with sides tangent to a circle [15]; (iv) Triangles associated with two lines and a point not on them [28], etc. (v) Stanev has describes the (ellptic) locus for the centroid of ellipse-inscribed equilaterals [29].

Some examples of polygon families include (i) rectangles inscribed in smooth curves [26], (ii) Poncelet polygons and the locus of their centroids [27] or their circumcenter [2].

We’ve studied loci of 3-periodics in the elliptic billiard, having found experimentally that the locus of the incenter is an ellipse [23]. This was subsequently proved [25]. Appearing thereafter were proofs for the elliptic locus of the barycenter [16] and circumcenter [5, 7]. More recently, with the help of a computer algebra system (CAS), we showed that 29 out of the first 100 entries in [13] are ellipses over billiard 3-periodics, though what determines ellipticity is still not understood [10]. We’ve

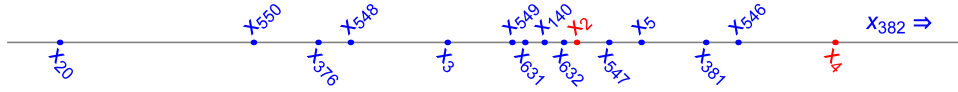


FIGURE 2. Relative locations of the first 16 triangle centers on [13] which are both on the Euler line and which are fixed affine combinations of  $X_2$  and  $X_4$ .

also studied properties (e.g., area invariance) of the negative pedal curve (NPC) of the ellipse with respect to a point on its boundary [11] as well as its pedal-like derivatives [24]. We have also studied the locus of Brocard points over circle- and ellipse-inscribed triangle families [8].

The envelope of Euler lines in triangles with two fixed vertices at the foci of an ellipse was studied in [17]. Note: we study loci of this family in Appendix C.

**Article Structure.** Section 2 defines basic concepts used in the article. Section 3 contains our main results. Section 4 analyzes loci over families of parallel  $V_1V_2$ . Section 5 analyzes the envelope of loci with fixed  $V_1$  and varying  $V_2$ . In the conclusion, Section 6, a table is included with videos mentioned throughout the paper. A set of appendices is included: Appendix C overviews triangle centers whose loci are ellipses for a closely-related triangle family:  $V_1V_2$  are fixed on the foci of  $\mathcal{E}$ . Appendix A includes longer calculations used in derivations of key properties of elliptic loci. Finally, Appendix D contains a quick-reference to most symbols used herein.

## 2. DEFINITIONS

Let  $(a, b)$  be the semi-axes of ellipse  $\mathcal{E}$  centered on  $O$ ,  $a \geq b$ . Let  $U(s) = [a \cos s, b \sin s]$  be a generic point on its boundary. Let  $t_1, t_2$  be two constants, and define  $V_1 = U(t_1)$ ,  $V_2 = U(t_2)$ . Consider the triangle family  $\mathcal{T}(t) = V_1V_2P(t)$ , where  $P(t) = U(t)$ ,  $t \in [0, 2\pi)$ ; see Figure 1.

Given a  $\mathcal{T}(t)$ , Let  $\mathcal{X}_\rho$  be a fixed affine combination of barycenter  $X_2$  and orthocenter  $X_4$  (both on Euler Line  $\mathcal{L}_e$ ), i.e.,  $\mathcal{X}_\rho = (1 - \rho)X_2 + \rho X_4$ ; Figure 2 depicts the relative locations of the first 16 centers on [13] with fixed  $\rho$ , whereas Table 1 specifies their respective  $\rho$ .

$X_k$	20	550	376	548	3	549	631	140	632	<b>2</b>	547	5	381	546	<b>4</b>	382
$\rho$	-2	-1.25	-1	-0.875	-0.5	-0.25	-0.2	-0.125	-0.05	<b>0</b>	0.125	0.25	0.5	0.625	<b>1</b>	2.5

TABLE 1. First 16 points on [13] on Euler line and at fixed  $\rho$ .

Currently, upwards of 38k+ *triangle centers* are catalogued in [13]. These are points on the plane of a triangle whose trilinear (or barycentric) coordinates are functions of side lengths and angles. Said functions must satisfy homogeneity, bisymmetry, and cyclicity [32, Triangle Center]. Examples include such classic centers as the incenter  $X_1$ , barycenter  $X_2$ , circumcenter  $X_3$ , orthocenter

*Remark 1.* Since  $\mathcal{X}_\rho$  is an affine combination of two triangle centers, its barycentrics add in a similar manner and therefore  $\mathcal{X}_\rho$  is also a triangle center [19].

Finally, let  $c^2 = a^2 - b^2$ ,  $d^2 = a^2 + b^2$ , and  $z = \cos(t_1 + t_2)$ .

## 3. MAIN RESULTS

Referring to Figure 1:

*Remark 2.* Since  $X_2 = [V_1 + V_2 + P(t)]/3$ , the locus of  $X_2$  is an ellipse  $\mathcal{E}_2$  centered on  $O_2 = (V_1 + V_2)/3$ , axis-parallel with  $\mathcal{E}$ , and with semi-axes  $(a_2, b_2) = (a/3, b/3)$ .

**Proposition 1.** *For any  $V_1, V_2$ , the locus of  $X_4$  is an ellipse  $\mathcal{E}_4$  of semi-axes  $a_4, b_4$ , centered on  $O_4$ , axis-parallel with  $\mathcal{E}$ , and with aspect ratio  $b/a$ . These are given by:*

$$O_4 = \frac{c^2}{2} \left[ \frac{\cos t_1 + \cos t_2}{a}, \frac{\sin t_1 + \sin t_2}{b} \right]$$

$$(a_4, b_4) = (w/a, w/b), \quad \text{where: } w = \frac{\sqrt{2}}{2} \left( \sqrt{a^4 + b^4 + (b^4 - a^4)z} \right)$$

*Proof.* Note that the pencils of sidelines  $V_1P(t)$  and  $V_2P(t)$  are invariant under projective transformations, and are respectively congruent to that of the altitudes  $V_2X_4$  and  $V_1X_4$ . Thus, Steiner's generation of conics [3] shows immediately that the locus of  $X_4$  is an ellipse similar to  $\mathcal{E}$ , but rotated  $90^\circ$ .

Using a CAS for simplification obtain the following parametric for  $\mathcal{E}_4$ :

$$\mathcal{E}_4 : [x_4(t), y_4(t)], t \in [0, 2\pi), \text{ where:}$$

$$x_4(t) = \frac{d^2(\cos t_1 + \cos t_2 + \cos t) + c^2 \cos(t_1 + t_2 + t)}{2a}$$

$$y_4(t) = \frac{d^2(\sin t_1 + \sin t_2 + \sin t) + c^2 \sin(t_1 + t_2 + t)}{2b}$$

□

**Theorem 1.** *For any  $V_1, V_2$ , and any  $\rho$ , the locus of  $\mathcal{X}_\rho$  is an ellipse (in general not axis-parallel with  $\mathcal{E}$ ) with parametric:*

$$\mathcal{E}_\rho : [x_\rho(t), y_\rho(t)], t \in [0, 2\pi), \text{ where:}$$

$$x_\rho = \frac{(a^2(\rho + 2) + 3b^2\rho)(\cos t_1 + \cos t_2 + \cos t)}{6a} - \frac{c^2\rho \cos(t + t_1 + t_2)}{2a}$$

$$y_\rho = \frac{(a^2(\rho + 2) + 3b^2\rho)(\sin t_1 + \sin t_2 + \sin t)}{6b} - \frac{c^2\rho \sin(t + t_1 + t_2)}{2b}$$

and center  $O_\rho$  at:

$$O_\rho = \left[ \frac{(a^2(\rho + 2) + 3b^2\rho)(\cos t_1 + \cos t_2)}{6a}, \frac{(3a^2\rho + b^2(\rho + 2))(\sin t_1 + \sin t_2)}{6b} \right]$$

*Proof.* CAS manipulation of  $\mathcal{X}_\rho = (1 - \rho)X_2 + \rho X_4$ . □

in Appendix B we've included all 226 triangle centers on [13] which are fixed affine combinations of  $X_2, X_4$ .

As before, let  $U(s)$  denote  $[a \cos s, b \sin s]$  on  $\mathcal{E}$ .

**Lemma 1.** *Lines  $U(t_1)U(t_2)$  are parallel for all  $t_1 + t_2 = t_0$ , where  $t_0$  is some constant.*

*Proof.* The slope of the line through points  $U(t_1) = [a \cos(t_1), b \sin(t_1)]$  and  $U(t_2) = [a \cos(t_2), b \sin(t_2)]$  is given by

$$\frac{b(\sin t_1 - \sin t_2)}{a(\cos t_1 - \cos t_2)} = \frac{2b \cos(\frac{t_1+t_2}{2}) \sin(\frac{t_1-t_2}{2})}{-2a \sin(\frac{t_1+t_2}{2}) \sin(\frac{t_1-t_2}{2})} = -\frac{b}{a} \cot\left(\frac{t_0}{2}\right)$$

which only depends on  $t_0$ .  $\square$

*Remark 3.* Lemma 1 implies that if  $V_1V_2$  are vertical (resp. horizontal), then  $t_1 + t_2 = 2k\pi$  (resp.  $t_1 + t_2 = (2k + 1)\pi$ ), where  $k$  is an integer.

**Corollary 1.** *For  $V_1V_2$  vertical or horizontal, for all  $\rho$ , the locus of  $\mathcal{X}_\rho$  is axis-parallel with  $\mathcal{E}$ .*

*Proof.* Follows from the implicit equation for  $\mathcal{X}_\rho$  (Appendix A). Specifically, the coefficient  $a_{11}$  of  $xy$  vanishes whenever  $t_1 + t_2$  is an integer multiple of  $\pi$ .  $\square$

Let  $(a_\rho, b_\rho)$  denote the semi-axes of the locus of  $\mathcal{X}_\rho$ .

**Proposition 2.** *The ratio  $a_\rho/b_\rho$  is invariant over the family of parallel  $V_1V_2$ .*

*Proof.* Rewrite the ellipse in Theorem 1 implicitly, and using a CAS obtain the ratio of eigenvalues of its Hessian, yielding the expression for  $a_\rho/b_\rho$  in Appendix A. Notice its non-constant terms only depend on the sum  $t_1 + t_2$  which with Lemma 1 yields the claim.  $\square$

**Corollary 2.** *For exactly three values of  $\rho$ , namely,  $0, 1/4, 1$  (corresponding to  $X_2, X_5$ , and  $X_4$ ), the aspect ratio of the corresponding elliptic locus is independent of  $V_1$  and  $V_2$ , i.e., it only depends on  $(a, b)$ .*

*Proof.* For  $\rho \in \{0, 1/4\}$  the aspect ratio is equal to  $a/b$  and for  $\rho = 1/4$  it is equal to  $(a^2 + b^2)/(2ab)$ . From Appendix A it follows that  $\lambda_\rho = a_\rho/b_\rho$  is a function of  $[\rho, \cos(t_1 + t_2)] = (\rho, z)$ . The function  $\lambda_\rho(\rho, z)$  is independent of  $z$  when the level set  $\partial\lambda_\rho/\partial z = 0$  is a vertical straight line. Direct analysis shows that is the case exactly when  $\rho \in \{0, 1/4, 1\}$ .  $\square$

**Proposition 3.** *The product  $a_\rho b_\rho$  is invariant over the family of parallel  $V_1V_2$  and given by:*

$$a_\rho b_\rho = \frac{|(2\rho + 1)(2a^2b^2(\rho - 1) + 3\rho(a^4 - b^4) \cos(t_1 + t_2) - 3\rho(a^4 + b^4))|}{18ab}$$

*Proof.* Obtain the above from Equation 1 in Appendix A. Since for parallel  $V_1V_2$ ,  $t_1 + t_2$  is constant (Lemma 1), the proof is complete. Alternatively, the same result could be obtained by symbolic simplification of the affine curvature of  $\mathcal{X}_\rho$  equal to  $(a_\rho b_\rho)^{-2/3}$ , since it is an ellipse [12].  $\square$

*Remark 4.* Only for  $\rho \in \{0, -1/2\}$ , i.e.,  $\mathcal{X}_\rho \in \{X_2, X_3\}$ , is the product  $a_\rho b_\rho$  independent of  $V_1V_2$ , and equal to  $ab/9$  and  $0$ , respectively.

**Corollary 3** (Axis annihilation). *For each family of parallel  $V_1V_2$ , there is a unique  $\rho$  (other than  $-1/2$ ) such that the product  $a_\rho b_\rho = 0$ . Said  $\rho$  is given by:*

$$\rho = \frac{2a^2b^2}{3(a^4 - b^4) \cos(t_1 + t_2) + 2a^2b^2 - 3a^4 - 3b^4}$$

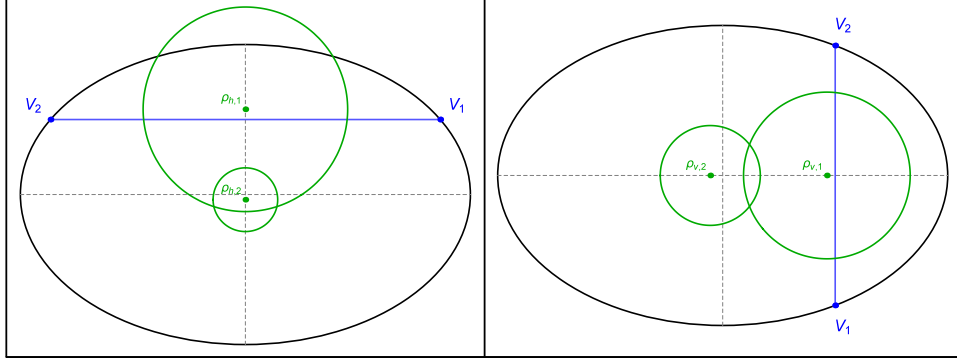


FIGURE 3. The loci of  $\mathcal{X}_\rho$  (green) can only be circles when  $V_1V_2$  (blue) are horizontal (left) or vertical (right). When horizontal (resp. vertical) only at  $\rho = \{\rho_{h,1}, \rho_{h,2}\}$  (resp.  $\rho = \{\rho_{v,1}, \rho_{v,2}\}$ ) is the locus a circle. As the  $V_1V_2$  traverse all horizontals (resp. verticals), the circles will rigidly translate vertically (resp. horizontally). [Video](#)

except when the denominator vanishes, which can only happen if  $a/b < \sqrt{3}$ . In this case, no  $\rho$  exists.

*Proof.* Follows from the expression for  $a_\rho b_\rho$  in Proposition 3.  $\square$

*Remark 5.* It  $a/b = \sqrt{3}$ , for vertical  $V_1V_2$ , the axis can't be annihilated.

Referring to Figure 4:

**Corollary 4.** *The semi-axis lengths  $a_\rho, b_\rho$  of the locus of  $\mathcal{X}_\rho$  are invariant over the family of parallel  $V_1V_2$ .*

*Proof.* By Proposition 2 and Lemma 3, the ratio  $a_\rho/b_\rho$  and product  $a_\rho b_\rho$  of the axes are invariant over parallel  $V_1V_2$ , respectively. The result follows.  $\square$

Referring to Figure 3:

**Proposition 4.** *The locus of  $\mathcal{X}_\rho$  is a circle iff  $V_1V_2$  is (i) horizontal with  $\rho$  assuming two values  $\rho_h$ , or (ii) vertical with  $a \neq 3b$ , and  $\rho$  assuming two values  $\rho_v$ . These are given by:*

$$\rho_h = \frac{b}{b \pm 3a}, \quad \rho_v = \frac{a}{a \pm 3b}$$

*Proof.* The parametrization for  $(x_\rho, y_\rho)$  in Theorem 1 can be developed to yield:

- For  $t_1 + t_2 = \pi$  and  $\rho = b/(b + 3a)$ ,  $\mathcal{X}_\rho$  is a circle centered in  $[0, (a + b)^2 \sin t_1 / (3a + b)]$  and radius  $a(a + b)/(b + 3a)$ .
- For  $t_1 + t_2 = \pi$  and  $\rho = b/(b - 3a)$ ,  $\mathcal{X}_\rho$  is a circle centered in  $[0, (a - b)^2 \sin t_1 / (b - 3a)]$  and radius  $a(a - b)/(3a - b)$ .
- For  $t_1 + t_2 = 0$  and  $\rho = a/(a + 3b)$ ,  $\mathcal{X}_\rho$  is a circle centered in  $[(a + b)^2 \cos t_1 / (a + 3b), 0]$  and radius  $b(a + b)/(a + 3b)$ .
- For  $t_1 + t_2 = 0$ ,  $\rho = a/(a - 3b)$  and  $a \neq 3b$ ,  $\mathcal{X}_\rho$  is a circle centered in  $[(a - b)^2 \cos t_1 / (a - 3b), 0]$  and radius  $|b(a - b)/(a - 3b)|$ .

If  $V_1V_2$  is neither horizontal nor vertical, there are no real solutions for  $\rho$  such that  $a_\rho/b_\rho = 1$ .  $\square$

**Proposition 5.** For  $V_1V_2$  vertical, consider the case of  $a = 3b$  and  $\rho \notin \{-1/2, 3/2\}$ . The locus of  $X_\rho$  is the axis-parallel ellipse centered at  $[2b(2r+3) \cos t_1/2, 0]$  and axes  $a_\rho = b|2r-3|/3$ ,  $b_\rho = b|2r+1|/3$ . This ellipse is a circle when  $\rho = 1/2$ , i.e., when  $X_\rho = X_{381}$ .

*Proof.* Direct derivation from Theorem 1.  $\square$

*Remark 6.* By definition,  $X_3$  is contained in the perpendicular bisector of  $V_1V_2$ , given by:

$$-2a \sin(t_1 + t_2)x + 2b(\cos(t_1 + t_2) + 1)y + c^2(\cos t_1 + \cos t_2) \sin(t_1 + t_2) = 0$$

**Proposition 6.** The locus of  $X_3$  is a variable-length segment  $P_3P'_3$  given by:

$$\begin{aligned} P_{3,x} &= \frac{c^2}{4a} \left( \frac{(1 - \cos(2t_1 + 2t_2))}{\sqrt{2 - 2 \cos(t_1 + t_2)}} + \cos t_1 + \cos t_2 \right) \\ P_{3,y} &= -\frac{c^2}{4b} \left( \sqrt{2 - 2 \cos(t_1 + t_2)} + \sin t_1 + \sin t_2 \right) \\ P'_{3,x} &= \frac{c^2}{4a} \left( \frac{(\cos(2t_1 + 2t_2) - 1)}{\sqrt{2 - 2 \cos(t_1 + t_2)}} + \cos t_1 + \cos t_2 \right) \\ P'_{3,y} &= \frac{c^2}{4b} \left( \sqrt{2 - 2 \cos(t_1 + t_2)} - \sin t_1 - \sin t_2 \right) \end{aligned}$$

Furthermore, its length  $L_3$  is given by:

$$L_3 = |P_3 - P'_3| = \frac{c^2 \sqrt{2(d^2 - c^2 \cos(t_1 + t_2))}}{2ab}$$

*Proof.* The coordinates of  $X_3 = [x_3, y_3]$  are given by:

$$\begin{aligned} x_3 &= \frac{c^2}{4a} (\cos(t + t_1 + t_2) + \cos t_1 + \cos t_2 + \cos t) \\ y_3 &= \frac{c^2}{4b} (\sin(t + t_1 + t_2) - \sin t_1 - \sin t_2 - \sin t) \end{aligned}$$

Direct calculations yield the claimed expressions.  $\square$

**Corollary 5.** The min (resp. max) of  $L_3$  is  $c^2/a$  (resp.  $c^2/b$ ) and the midpoint of  $P_3P'_3$  is given by

$$\left[ \frac{c^2}{4a} (\cos t_1 + \cos t_2), -\frac{c^2}{4b} (\sin t_1 + \sin t_2) \right]$$

*Proof.* Direct from the Proposition 6.  $\square$

#### 4. LOCUS CENTER TRANSLATION

Referring to Figure 4:

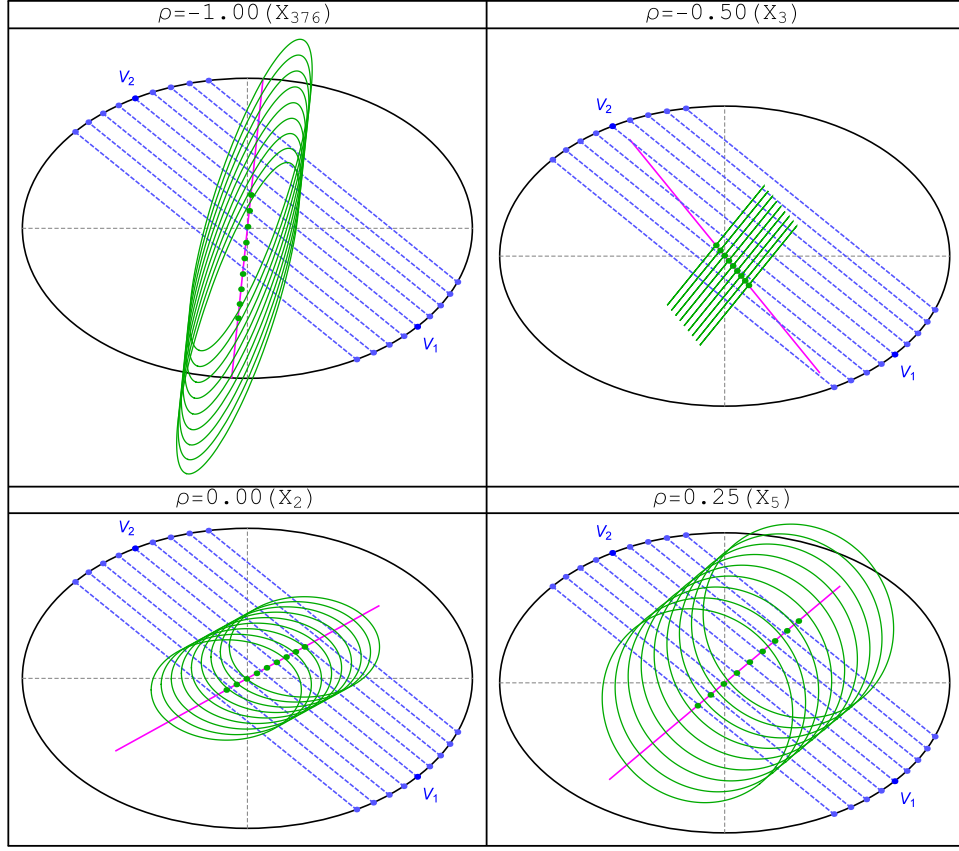


FIGURE 4. Over the family of parallel  $V_1V_2$  (dashed blue, constant  $t_1 + t_2$ ), the loci of  $\mathcal{X}_\rho$  (solid green) are a family of rigidly-translating ellipses. Their centers (green dots) move along a straight line  $\mathcal{L}_\parallel$  (magenta) which crosses  $\mathcal{E}$ 's center. Shown are the cases for  $\rho \in \{-1, -1/2, 0, 1/4\}$ , i.e.,  $X_k, k = 376, 3, 2, 5$ , respectively. [Video](#)

**Proposition 7.** *Over the family of parallel  $V_1V_2$ , the locus of  $\mathcal{X}_\rho$  is a family of rigidly-translating ellipses whose center moves along a straight line  $\mathcal{L}_\parallel$  passing through  $O$  and given by:*

$$\mathcal{L}_\parallel : y = \frac{a}{b} \cdot \frac{(3a^2 + b^2)\rho + 2b^2}{(a^2 + 3b^2)\rho + 2a^2} \tan\left(\frac{t_1 + t_2}{2}\right) x$$

*Proof.* Directly from the expression for  $O_\rho$  in Theorem 1. □

*Remark 7.*  $\mathcal{L}_\parallel$  is perpendicular to  $V_1V_2$  when  $\rho = 1$  ( $X_4$ ).

Referring to Figure 5:

**Proposition 8.** *For  $V_1V_2$  stationary, as one varies  $\rho$ , the center  $O_\rho$  of the locus of  $\mathcal{X}_\rho$  follows a straight line  $\mathcal{L}_\rho$  whose slope only depends on the slope of  $V_1V_2$ . In*



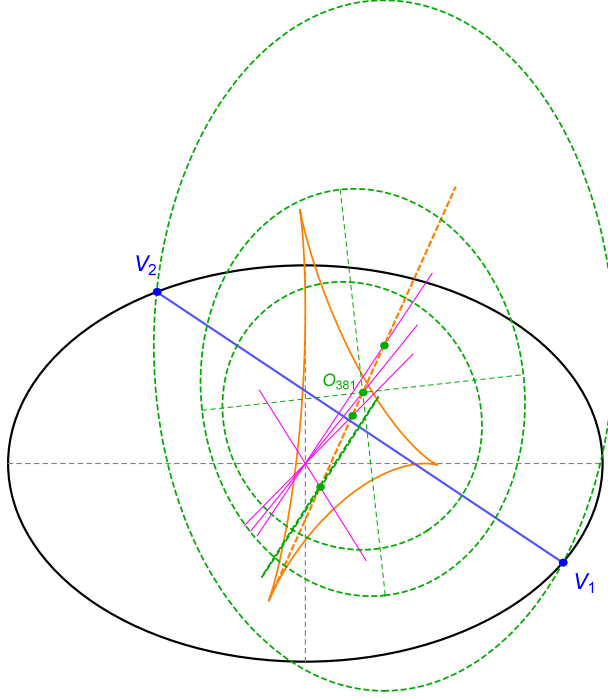


FIGURE 5. Elliptic loci (green ellipses) are shown for  $\rho \in \{0, 1/4, 1/2, 1\}$  with centers  $O_k, k = 2, 5, 381, 4$  on a line  $\mathcal{L}_\rho$  (dashed orange). Also shown is a family of lines  $\mathcal{L}_\parallel$  (magenta) passing through the center of  $\mathcal{E}$  depicting the locus of individual  $O_\rho$  as the family of parallel  $V_1V_2$  is traversed. Also shown (solid orange) is the tricuspoid envelope of  $\mathcal{L}_\rho$  for fixed  $V_1$ , over all  $V_2$  on  $\mathcal{E}$ . [Video](#)

fact:

$$\mathcal{L}_\rho : \left[ \frac{a(\cos t_1 + \cos t_2)}{3}, \frac{b(\sin t_1 + \sin t_2)}{3} \right] + \\ + \rho \cos\left(\frac{t_1 - t_2}{2}\right) \left[ \frac{a^2 + 3b^2}{3a} \cos\left(\frac{t_1 + t_2}{2}\right), \frac{3a^2 + b^2}{3b} \sin\left(\frac{t_1 + t_2}{2}\right) \right]$$

*Proof.* Follows from Theorem 1.  $\square$

**Corollary 6.** *The product of the slopes of  $\mathcal{L}_\rho$  and  $V_1V_2$  is constant over all choices of  $V_1$  and  $V_2$  and equal to  $-\frac{3a^2+b^2}{a^2+3b^2}$ .*

**Corollary 7.** *Only when  $V_1V_2$  coincides with either the major or minor axis of  $\mathcal{E}$  can  $\mathcal{L}_\rho$  pass through the center of  $\mathcal{E}$ .*

Referring to Figure 6 (bottom right):

*Remark 8.* When  $V_1V_2$  passes thru  $O$ ,  $\mathcal{L}_\rho$  collapses to  $O$ , and  $O_\rho = O$  for all  $\rho$ .

**Corollary 8.**  *$O_\rho$  is on  $V_1V_2$  at the following  $\rho$ :*

$$\rho = \frac{2a^2b^2}{3(b^4 - a^4)\cos(t_1 + t_2) + 2a^2b^2 + 3a^4 + 3b^4}$$

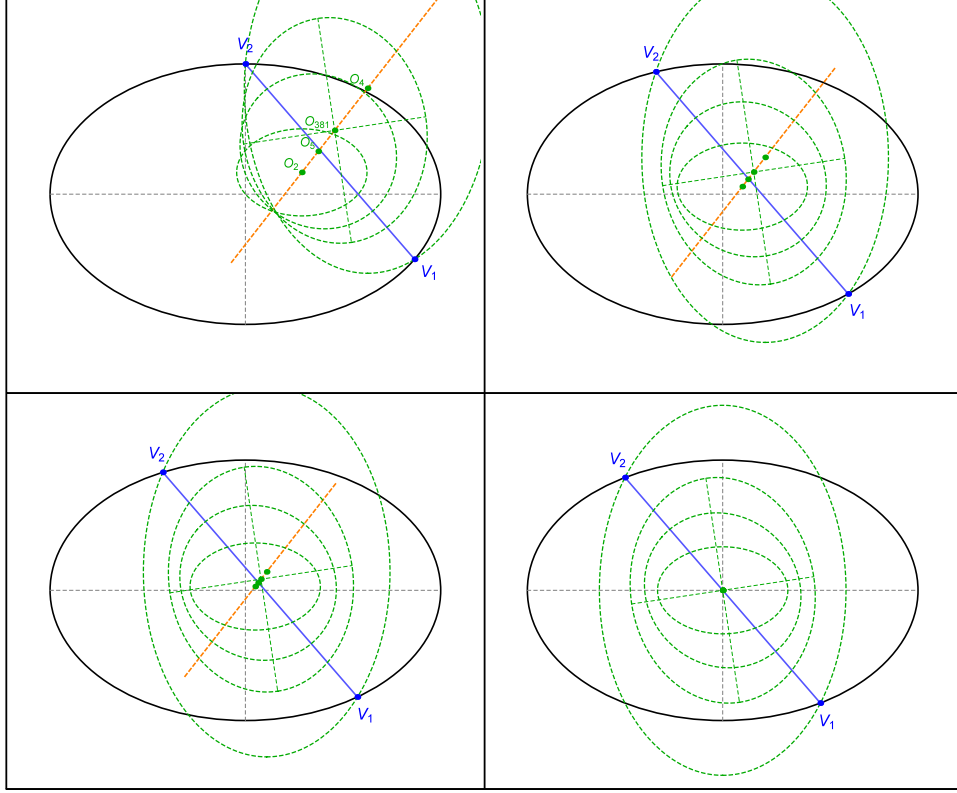


FIGURE 6. Four positions of parallel  $V_1V_2$  are shown, approaching the center of  $\mathcal{E}$ . For each position, loci for  $\rho = \{0, 1/4, 1/2, 1\}$  are collinear on  $\mathcal{L}_\rho$  (dashed orange). Notice as  $V_1V_2$  approaches the position where it crosses the origin, centers come closer to each other and  $\mathcal{L}_\rho$  degenerates to a point (bottom right). [Video](#)

## 5. PHENOMENA WITH $V_1$ FIXED AND $V_2$ VARIABLE

### 5.1. Envelope of $\mathcal{L}_\rho$ . Referring to Figure 5:

**Proposition 9.** *For fixed  $V_1$ , over all  $V_2$  on  $\mathcal{E}$ , the envelope of  $\mathcal{L}_\rho$  is a 3-cusped quartic curve  $\Delta$  affine to Steiner's deltoid, given parametrically by:*

$$\begin{aligned} \Delta_{t_1}(u) = & \left[ \frac{\cos t_1 (a^4 - b^4)}{2a(3a^2 + b^2)}, -\frac{\sin t_1 (a^4 - b^4)}{2b(a^2 + 3b^2)} \right] \\ & + \left[ \frac{(2 \cos u + \cos(t_1 + 2u))(a^4 - b^4)}{2a(3a^2 + b^2)}, -\frac{(2 \sin u - \sin(t_1 + 2u))(a^4 - b^4)}{2b(a^2 + 3b^2)} \right] \end{aligned}$$

*Proof.* Follows from Proposition 8 and the definition of the envelope [12, Chapt. 3].  $\square$

**Proposition 10.** *The area of the region bounded by  $\Delta_{t_1}$  is invariant over  $t_1$  and given by*

$$A(\Delta_{t_1}) = \frac{\pi(a^4 - b^4)^2}{ab(3a^2 + b^2)(a^2 + 3b^2)}$$

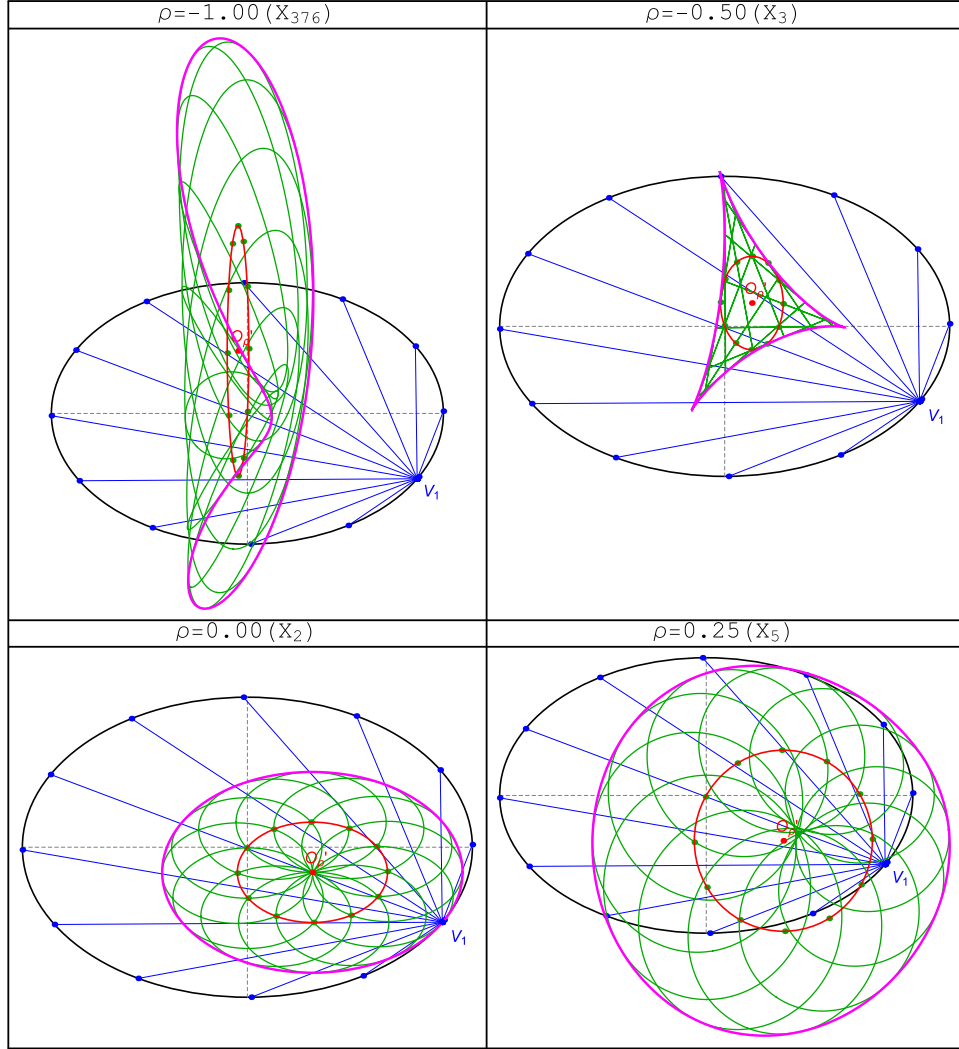


FIGURE 7. For a choice of  $V_1$  and over  $V_2$  on  $\mathcal{E}$  (black), the loci of  $\mathcal{X}_\rho$  are a family of ellipses (green) whose centers (green dots) sweep an ellipse  $\Gamma_\rho$  passing through the center of  $\mathcal{E}$  and centered  $O'_\rho$ . Shown are the cases for  $\rho \in \{-1, -1/2, 0, 1/4\}$ , i.e.,  $X_k$ ,  $k = 376, 3, 2, 5$ , respectively. Also shown are envelopes (pink) to the ellipse families. For  $X_3$  (top right), the envelope is a half-sized Steiner's hat [11]; for  $X_2$  (bottom left) the envelope is an ellipse of fixed axes, internally tangent to  $\mathcal{E}$  at one point. All envelopes are area-invariant wrt  $V_1$ .

5.2. Locus of  $O_\rho$ . Referring to Figure 7:

**Proposition 11.** *With  $V_1$  fixed, over all  $V_2$ , the locus of centers  $O_\rho$  of the loci of  $\mathcal{X}_\rho$  is an ellipse  $\Gamma_\rho$  centered on  $O'_\rho$ , which is axis-parallel with  $\mathcal{E}$  and contains its center  $O$ . Its semiaxes  $(a', b')$  and center are given by:*

$$(a', b') = \left( \frac{a^2(\rho + 2) + 3b^2\rho}{6a}, \frac{3a^2\rho + b^2(\rho + 2)}{6b} \right)$$

$$O'_\rho = [a' \cos t_1, b' \sin t_1]$$

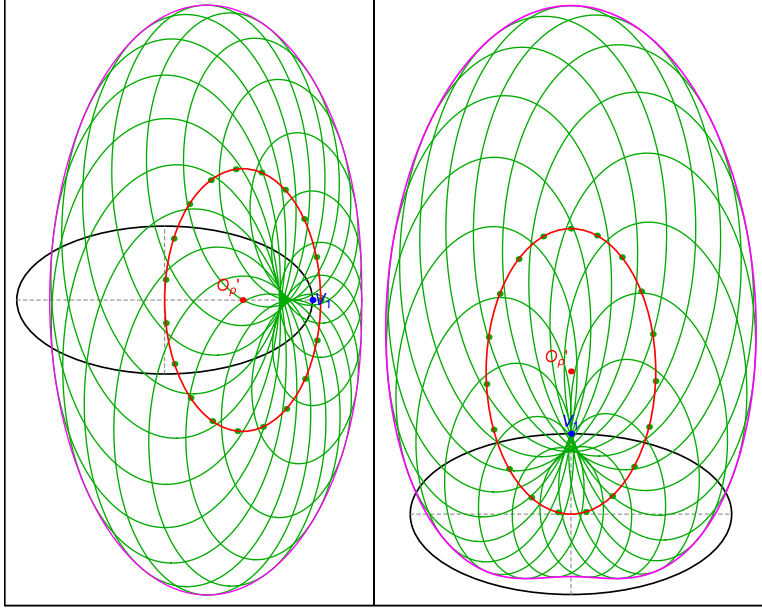


FIGURE 8. Locus  $\Gamma_\rho$  (red) of the centers of  $\mathcal{X}_\rho$  (green) of  $\mathcal{X}_\rho$  for  $\rho = 2/3$ , when  $V_1$  coincides with the left (resp. top) vertex of  $\mathcal{E}$  (black). Notice  $\Gamma_\rho$  (red) is tangent at the center of  $O$  to the minor (resp. major) axis of  $\mathcal{E}$  and its center  $O'_\rho$  lies on the major (resp. minor) axis of  $\mathcal{E}$ .

**Corollary 9.** At  $\rho = 1$  ( $X_4$ ),  $\Gamma_\rho$  is an axis-parallel ellipse with aspect ratio  $b/a$  with center at  $\left[ \frac{(a^2+b^2)\cos t_1}{2a}, \frac{(a^2+b^2)\sin t_1}{2b} \right]$  and axes  $\left( \frac{a^2+b^2}{2a}, \frac{a^2+b^2}{2b} \right)$ .

**Corollary 10.** At  $\rho = 0$  ( $X_2$ ),  $\Gamma_\rho$  is an ellipse with aspect ratio  $a/b$  centered at  $\left[ \frac{1}{3}a \cos t_1, \frac{1}{3}b \sin t_1 \right]$  with axes  $\left( \frac{a}{3}, \frac{b}{3} \right)$ .

**Corollary 11.** Over all  $V_1$  the locus of  $O'_\rho$  is an ellipse  $\Gamma'_\rho$  which is axis-parallel and concentric with  $\mathcal{E}$ . The semi-axes of  $\Gamma'_\rho$  are also  $(a', b')$ .

Referring to Figure 8:

*Remark 9.* If  $V_1$  is fixed at the left (resp. top) vertex of  $\mathcal{E}$ , over all  $V_2$ ,  $\Gamma_\rho$  is axis-parallel with  $\mathcal{E}$  and tangent at  $O$  to its minor (resp. major) axis.

### 5.3. Envelope of the family of elliptic $\mathcal{X}_\rho$ .

**Proposition 12.** With  $V_1$  stationary and  $V_2$  sweeping the boundary of  $\mathcal{E}$ , a regular part of the envelope of  $\mathcal{X}_\rho$  is a curve  $\Gamma_{t_1}$  parametrized by

$$x_{t_1} = \frac{[(a^2 + 3b^2)(2 \cos t + \cos t_1) - 3c^2 \cos(t_1 + 2t)]\rho}{6a} + \frac{a}{3}(2 \cos t + \cos t_1)$$

$$y_{t_1} = \frac{[(3a^2 + b^2)(2 \sin t + \sin t_1) - 3c^2 \sin(t_1 + 2t)]\rho}{6b} + \frac{b}{3}(2 \sin t + \sin t_1)$$

*Proof.* Direct from the definition of an envelope [12] via CAS simplification.  $\square$

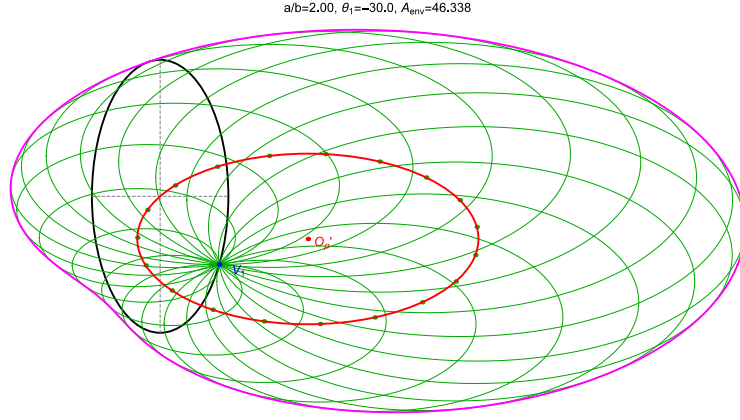


FIGURE 9. Let  $V_1$  be a point on  $\mathcal{E}$  (black, rotated 90 degrees to save space,  $a/b = 2$ ). Over  $V_2$ , the loci of  $X_4$  are ellipses (green) which all pass through  $V_1$ . Their centers (green dots) sweep an axis-parallel ellipse (red) centered at  $O'_\rho$ , whose aspect ratio is  $b/a$ . The exterior envelope of said loci is (in general) a non-convex curve (pink) which is the affine image of Pascal's Limaçon. Its area is independent of  $V_1$ , and it is tangent to  $\mathcal{E}$  at at least one point. [Video](#)

**Proposition 13.** *The area (algebraic) of the region bounded by  $\Gamma_{t_1}$  is invariant over  $t_1$  and given by*

$$A(\Gamma_{t_1}) = \frac{\pi}{9} \left[ \frac{(15a^4 + 2a^2b^2 + 15b^4)\rho^2}{2ab} + \frac{2(3a^4 + 2a^2b^2 + 3b^4)\rho}{ab} + 4ab \right]$$

*Proof.* Follows by direct integration of  $A(\Gamma_{t_1}) = \frac{1}{2} \int_{\Gamma_{t_1}} (xdy - ydx)$ .  $\square$

In [11] we called *Steiner's Hat* the negative pedal curve of an ellipse with respect to a point  $M$  on the boundary. One of its curious properties is that it is area-invariant over all  $M$ .

*Remark 10.* With  $V_1$  stationary and  $V_2$  sweeping the boundary of  $\mathcal{E}$ , the envelope of the locus of  $X_3$  over all positions of  $V_2$  is 2:1 homothetic to Steiner's Hat.

This stems from the fact that it cuts  $V_1V_2$  perpendicularly and at its midpoint. Referring to Figure 7 (bottom left) and Figure 9:

*Remark 11.* For  $\rho = 0$  (resp.  $\rho = 1$ ), the external envelope of  $\mathcal{X}_\rho$  is internally (resp. externally) tangent to  $\mathcal{E}$  at  $V_1$  (resp. at the point(s) on  $\mathcal{E}$  whose normal goes through  $V_1$ ). For  $\rho = 0$  the envelope is elliptic with axes  $2a/3$  and  $2b/3$ .

**Proposition 14.** *For  $\rho = 1$ , the external envelope of  $\mathcal{X}_\rho$  is the affine image of Pascal's Limaçon.*

*Proof.* A construction for Pascal's Limaçon is given in [32, Pascal's Limaçon] as follows: specify a fixed point  $P$  and a circle  $C$ . Then draw all circles with centers on  $C$  which pass through  $P$ . The external envelope of said circles is the Limaçon. Referring to Figure 9, apply an affine transformation that sends  $\Gamma_\rho$  to a circle  $C$ . This will automatically send all  $\mathcal{X}_\rho$  ellipses to (variable radius) circles, since they have the same aspect ratio and are axis-parallel with  $\Gamma_\rho$  (Proposition 11). Therefore, the affine image of the  $\mathcal{X}_\rho$  becomes a family of circles with centers on  $C$  through a common point  $P$ , the affine image of  $V_1$ .  $\square$

## 6. CONCLUSION

This article studied properties of the loci of triangle centers over of a special of ellipse-inscribed triangles. The following questions are still unanswered:

- Is there a triangle center which is not a fixed affine combination of  $X_2, X_4$  whose locus over  $\mathcal{T}(t)$  is an ellipse? We did not find one amongst all 38k+ centers listed in [13].
- For  $V_1$  fixed and over all  $V_2$  on  $\mathcal{E}$ , are there interesting properties of the internal envelope of the family of  $\mathcal{X}_\rho$  ellipses? For  $X_2, X_4$ , this envelope is a point  $(O + (V_1 - O)/3)$ , and  $V_1$ , respectively. However for other  $\rho$  this envelope is more complex.

Animations illustrating the dynamic geometry of some of the above phenomena appear on Table 2.

Id	Title	youtu.be/...
01	Basic elliptic loci	<a href="https://youtu.be/zjiNgfndBWg">zjiNgfndBWg</a>
02	$\mathcal{X}_\rho$ slides on Euler line	<a href="https://youtu.be/w5KuN_OrQBQ">w5KuN_OrQBQ</a>
03	Locus of $\mathcal{X}_\rho$ over parallel $V_1V_2$	<a href="https://youtu.be/zFOeENDJRho">zFOeENDJRho</a>
04	Relative motion of loci over parallel $V_1V_2$	<a href="https://youtu.be/TpBjKlkFjkg">TpBjKlkFjkg</a>
05	Circular loci if $V_1V_2$ are horiz. or vert.	<a href="https://youtu.be/nLeKvxcicNY">nLeKvxcicNY</a>
06	Limaçon-Like envelopes of $X_4$ locus family	<a href="https://youtu.be/sPQrz7ddRfA">sPQrz7ddRfA</a>

TABLE 2. Illustrative animations, click on the link to view it on YouTube and/or enter [youtu.be/<code>](https://youtu.be/<code>) as a URL in your browser, where <code> is the provided string.

We are very grateful to A. Akopyan and P. Moses for key insights. We thank the journal referees for their valuable suggestions. We thank P.N. de Souza for his crucial editorial help. The second author is fellow of CNPq and coordinator of Project PRONEX/ CNPq/ FAPEG 2017 10 26 7000 508.

APPENDIX A. AXIS RATIO OF LOCUS OF  $\mathcal{X}_\rho$ 

Here we assume the origin is at the center of the  $\mathcal{X}_\rho$  locus. Then the latter can be expressed as:

$$\mathcal{X}_\rho : a_{20}x_1^2 + 2a_{11}x_1y_1 + a_{02}y_1^2 + a_{00} = 0$$

The aspect ratio is given by:

$$\frac{a_\rho}{b_\rho} = \frac{a_{20} + a_{02} + \sqrt{(a_{20} - a_{02})^2 + 4a_{11}^2}}{2(a_{20}a_{02} - a_{11}^2)}$$

The product of axes is given by:

$$(1) \quad a_\rho b_\rho = \frac{|a_{00}|}{\sqrt{a_{20}a_{02} - a_{11}^2}}$$

where (recall  $z = \cos(t_1 + t_2)$ ):

$$\begin{aligned} a_{20} &= 54a^2\rho c^2(3a^2\rho + b^2\rho + 2b^2)z \\ &\quad - 18a^2(9a^4 - 6b^2a^2 + 5b^4)\rho^2 - 36a^2b^2(3a^2 + b^2)\rho - 36a^2b^4 \\ a_{11} &= 54\rho(\rho - 1)abc^4\sqrt{1 - z^2} \\ a_{02} &= 54b^2\rho c^2(a^2\rho + 3b^2\rho + 2a^2)z \\ &\quad - 18b^2(5a^4 - 6b^2a^2 + 9b^4)\rho^2 - 36b^2(a^2 + 3b^2)a^2\rho - 36b^2a^4 \\ a_{00} &= (2\rho + 1)^2(3a^4\rho z - 3b^4\rho z - 3a^4\rho + 2a^2b^2\rho - 3b^4\rho - 2b^2a^2)^2 \end{aligned}$$

#### APPENDIX B. TRIANGLE CENTERS AT FIXED $\rho$

Amongst the 4.9k triangle centers on the Euler line [14], only the following 226 are fixed affine combinations of  $X_2$  and  $X_4$ :  $X_k, k = 2, 3, 4, 5, 20, 140, 376, 381, 382, 546, 547, 548, 549, 550, 631, 632, 1564, 1656, 1657, 2041, 2042, 2043, 2044, 2045, 2046, 2675, 2676, 3090, 3091, 3146, 3522, 3523, 3524, 3525, 3526, 3528, 3529, 3530, 3533, 3534, 3543, 3545, 3627, 3628, 3830, 3832, 3839, 3843, 3845, 3850, 3851, 3853, 3854, 3855, 3856, 3857, 3858, 3859, 3860, 3861, 5054, 5055, 5056, 5059, 5066, 5067, 5068, 5070, 5071, 5072, 5073, 5076, 5079, 7486, 8703, 10109, 10124, 10299, 10303, 10304, 11001, 11539, 11540, 11541, 11737, 11812, 12100, 12101, 12102, 12103, 12108, 12811, 12812, 14093, 14269, 14782, 14783, 14784, 14785, 14813, 14814, 14869, 14890, 14891, 14892, 14893, 15022, 15640, 15681, 15682, 15683, 15684, 15685, 15686, 15687, 15688, 15689, 15690, 15691, 15692, 15693, 15694, 15695, 15696, 15697, 15698, 15699, 15700, 15701, 15702, 15703, 15704, 15705, 15706, 15707, 15708, 15709, 15710, 15711, 15712, 15713, 15714, 15715, 15716, 15717, 15718, 15719, 15720, 15721, 15722, 15723, 15759, 15764, 15765, 16239, 16249, 16250, 16446, 17504, 17538, 17578, 17800, 18585, 18586, 18587, 19708, 19709, 19710, 19711, 21734, 21735, 23046, 33699, 33703, 33923, 34200, 34551, 34552, 34559, 34562, 35018, 35381, 35382, 35384, 35400, 35401, 35402, 35403, 35404, 35405, 35406, 35407, 35408, 35409, 35410, 35411, 35412, 35413, 35414, 35415, 35416, 35417, 35418, 35419, 35420, 35421, 35434, 35435, 35732, 35734, 35735, 35736, 35737, 35738, 36436, 36437, 36438, 36439, 36445, 36448, 36454, 36455, 36456, 36457, 36463, 36466.$

#### APPENDIX C. FOCUS-MOUNTED TRIANGLES

Consider the 1d family of triangles  $\mathcal{T}_f(t) = f_1f_2P(t)$  where  $P(t)$  sweeps  $\mathcal{E}$  and the  $f_j$  are the foci of  $\mathcal{E}$ , at  $[\pm c, 0]$ . Referring to Figure 10, noting that the result for  $X_1, X_2$  were proved in [4, Thm 2.2.1]:

**Proposition 15.** *Over the first 1000 triangle centers listed in [13], only the loci of  $X_k, k = 1, 2, 8, 10, 145, 551$  over  $\mathcal{T}_f(t)$  are ellipses. The first four are given by:*

$$\begin{aligned} X_1 &: \frac{x^2}{c^2} + \frac{(a+c)^2 y^2}{b^2 c^2} - 1 = 0 \\ X_2 &: \frac{9x^2}{a^2} + \frac{9y^2}{b^2} - 1 = 0 \\ X_8 &: \frac{x^2}{(a-2c)^2} + \frac{y^2(a+c)^2}{b^2(a-c)^2} - 1 = 0 \\ X_{10} &: \frac{4x^2}{(a-c)^2} + \frac{4(a+c)^2 y^2}{a^2 b^2} - 1 = 0 \end{aligned}$$

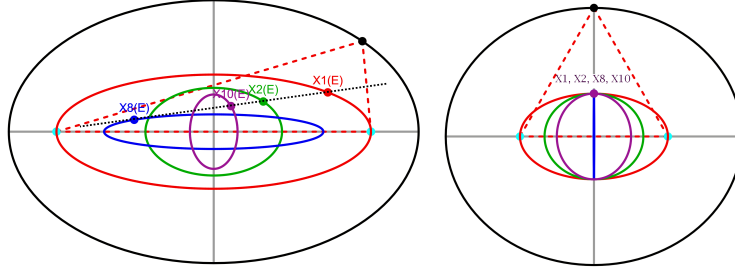


FIGURE 10. **Left:** elliptic loci of  $X_k, k = 1, 2, 8, 10$  (collinear on the Nagel line, dashed black) for a triangle family (dashed red) with two vertices on the foci. [animation 1](#) **Right:** at  $a/b = 2/\sqrt{3} \simeq 1.1547$ , the family contains two equilaterals (one shown dashed red), and therefore all loci are tangent at two points. Also at this  $a/b$ , the locus of  $X_8$  (blue) is a vertical segment. [animation 2](#)

*Remark 12.* The vertices of the locus of  $X_1$  are  $f_1, f_2$ .

*Remark 13.* At  $a = 2c$ , i.e.,  $a/b = 2/\sqrt{3} \simeq 1.1547$ , the locus of  $X_8$  is the vertical segment  $[0, \pm b/3]$ . At this aspect ratio, when  $P(t)$  is at the top or bottom vertex of  $\mathcal{E}$ ,  $\mathcal{T}_f(t)$  is equilateral.

Recall Line  $X_1X_2$  is known as the *Nagel Line* [14]. For the entire 40k+ centers in [13], the following 62 are fixed affine combinations of  $X_1, X_2$  (boldface indicates those in Proposition 15): **1, 2, 8, 10, 145, 551**, 1125, 1698, 3241, 3244, 3616, 3617, 3621, 3622, 3623, 3624, 3625, 3626, 3632, 3633, 3634, 3635, 3636, 3679, 3828, 4668, 4669, 4677, 4678, 4691, 4701, 4745, 4746, 4816, 5550, 9780, 15808, 19862, 19872, 19875, 19876, 19877, 19878, 19883, 20014, 20049, 20050, 20052, 20053, 20054, 20057, 22266, 25055, 31145, 31253, 34595, 34641, 34747, 36440, 36444, 36458, 36462.

Note that  $X_2$  is the anticomplement of itself. Note also that  $X_{10}$  (resp.  $X_{145}$ ) is the anticomplement of  $X_1$  (resp.  $X_8$ ). Numerically analyzing the loci of all 38k+ on [13] which are not on the  $X_1X_2$  line we found none which produced an ellipse over  $\mathcal{T}_f(t)$ . In turn this leads to the following conjecture:

**Conjecture 1.** *The locus of  $X_k$  over  $\mathcal{T}_f(t) = f_1f_2P(t)$  is an ellipse iff  $X_k$  is a fixed affine combination of  $X_1$  and  $X_2$ .*

#### APPENDIX D. TABLE OF SYMBOLS

Symbols used in the article appear on Table 3.



symbol	meaning
$\mathcal{E}, a, b$	base ellipse and its semi-axes
$O, f_1, f_2$	center of foci of $\mathcal{E}$
$V_1, V_2$	points fixed on $\mathcal{E}$ at $t_1, t_2$
$P(t)$	moving 3rd vertex of $\mathcal{T}$
$\mathcal{T}(t)$	$\mathcal{E}$ -inscribed triangle $V_1V_2P(t)$
$\mathcal{L}_e$	Euler line $X_2X_4$
$\mathcal{X}_\rho, \rho$	$\mathcal{X}_\rho = X_2 + \rho(X_4 - X_2)$
$c^2, d^2$	$a^2 - b^2$ , and $a^2 + b^2$ , resp.
$z$	shorthand for $\cos(t_1 + t_2)$
$O_\rho$	center of elliptic locus of $\mathcal{X}_\rho$
$\mathcal{L}_\rho, \mathcal{L}_\parallel$	linear locus of $O_\rho$ over $\rho$ (resp. $V_1V_2$ parallels)
$\Delta_{t_1}$	envelope of $\mathcal{L}_\rho$ for fixed $V_1$ over $V_2$ on $\mathcal{E}$
$\Gamma_\rho$	elliptic locus of $O_\rho$ for fixed $V_1$ over $V_2$ on $\mathcal{E}$
$O'_\rho, \Gamma'_\rho$	center of $\Gamma_\rho$ and its elliptic locus over all $V_1$ on $\mathcal{E}$
$X_1, X_2$	incenter, barycenter
$X_3, X_4$	circumcenter, orthocenter
$X_5, X_8$	9-pt circle center and Nagel point
$X_{10}, X_{381}$	Spieker center and $X_2X_4$ midpoint

TABLE 3. Symbols used in the article.

## REFERENCES

- [1] Akopyan, A. (2020). Locus of  $x_\rho$  is an ellipse if it lies on the Euler line at fixed affine combination of  $x_2, x_4$ . Private Communication.
- [2] Chavez-Caliz, A. (2021). More about areas and centers of Poncelet polygons. *Arnold Math J.*, 7: 91–106.
- [3] Coxeter, H. S. (1993). *The Real Projective Plane*. New York: Springer-Verlag.
- [4] Dykstra, J., Peterson, C., Rall, A., Shaddock, E. (2006). Orbiting vertex: Follow that triangle center! [bit.ly/2JaWMK9](https://bit.ly/2JaWMK9).
- [5] Fierobe, C. (2021). On the circumcenters of triangular orbits in elliptic billiard. *J. Dyn. Control Syst.* doi:10.1007/s10883-021-09537-2.
- [6] Gallatly, W. (1913). *The Modern Geometry of the Triangle*. London: Hodgson.
- [7] Garcia, R. (2019). Elliptic billiards and ellipses associated to the 3-periodic orbits. *American Mathematical Monthly*, 126(06): 491–504.
- [8] Garcia, R., Reznik, D. (2020). Loci of the Brocard points over selected triangle families. arXiv:2009.08561.
- [9] Garcia, R., Reznik, D. (2021). Related by similarity I: Poristic triangles and 3-periodics in the elliptic billiard. *Intl. J. of Geom.*, 10(3): 52–70.
- [10] Garcia, R., Reznik, D., Koiller, J. (2020). Loci of 3-periodics in an elliptic billiard: why so many ellipses? arXiv:2001.08041.
- [11] Garcia, R., Reznik, D., Stachel, H., Helman, M. (2020). Steiner's hat: a constant-area deltoid associated with the ellipse. *J. Croatian Soc. for Geom. Gr. (KoG)*, 24: 12–28.
- [12] Guggenheimer, H. (1977). *Differential Geometry*. New York: Dover.
- [13] Kimberling, C. (2019). Encyclopedia of triangle centers. [faculty.evansville.edu/ck6/encyclopedia/ETC.html](https://faculty.evansville.edu/ck6/encyclopedia/ETC.html).
- [14] Kimberling, C. (2020). Central lines of triangle centers. [bit.ly/34vVoJ8](https://bit.ly/34vVoJ8).
- [15] Kovačević, N., Šlipečević, A. (2012). On the certain families of triangles. *KoG-Zagreb*, 16: 21–27.
- [16] Levi, M., Tabachnikov, S. (2007). The Poncelet grid and billiards in ellipses. *The American Mathematical Monthly*, 114(10): 895–908. doi.org/10.1080/00029890.2007.11920482.
- [17] MacQueen, M. L., Hartley, R. W. (1946). Elliptic Euleroids. *Amer. Math. Monthly*, 53: 511–516. <https://doi.org/10.2307/2305067>.
- [18] Monroe, D., Blue (2019). Locus of orthocenter of triangle inscribed in ellipse. [bit.ly/2T60qFh](https://bit.ly/2T60qFh). Stack Exchange.

- [19] Moses, P. (2020). An affine combination of two triangle centers is a triangle center. Private Communication.
- [20] Murnaghan, F. D. (1925). Discussions: Note on Mr. Weaver's paper "a system of triangles related to a poristic system" (1924, 337–340). *Amer. Math. Monthly*, 32(1): 37–41. [www.jstor.org/stable/2300090](http://www.jstor.org/stable/2300090).
- [21] Odehnal, B. (2011). Poristic loci of triangle centers. *J. Geom. Graph.*, 15(1): 45–67.
- [22] Pamfilos, P. (2011). Triangles with given incircle and centroid. *Forum Geometricorum*, 11: 27–51.
- [23] Reznik, D. (2011). The locus of the incenter over 3-periodics in the elliptic billiard is an ellipse. YouTube. [youtu.be/BBsyM7RnswA](https://youtu.be/BBsyM7RnswA).
- [24] Reznik, D., Garcia, R., Stachel, H. (2020). Area-invariant pedal-like curves derived from the ellipse. Submitted, arXiv:2009.02581.
- [25] Romaskevich, O. (2014). On the incenters of triangular orbits on elliptic billiards. *Enseign. Math.*, 60(3-4): 247–255.
- [26] Schwartz, R. (2019). Rectangle coincidences and sweepouts. [arxiv.org/abs/1809.03070](https://arxiv.org/abs/1809.03070).
- [27] Schwartz, R., Tabachnikov, S. (2016). Centers of mass of Poncelet polygons, 200 years after. *Math. Intelligencer*, 38(2): 29–34.
- [28] Sliepčević, A., Halas, H. (2013). Family of triangles and related curves. *Hrvat. Akad. Znan. Umjet. Mat. Znan*, 17(515): 203–2010.
- [29] Stanev, M. (2019). Locus of the centroid of the equilateral triangle inscribed in an ellipse. *International Journal of Computer Discovered Mathematics (IJCDM)*, 4. [bit.ly/371XH4v](https://bit.ly/371XH4v).
- [30] Weaver, J. H. (1924). A system of triangles related to a poristic system. *Amer. Math. Monthly*, 31(7): 337–340. [www.jstor.org/stable/2299387](http://www.jstor.org/stable/2299387).
- [31] Weaver, J. H. (1933). Curves determined by a one-parameter family of triangles. *Amer. Math. Monthly*, 40(2): 85–91. [www.jstor.org/stable/2300940](http://www.jstor.org/stable/2300940).
- [32] Weisstein, E. (2019). Mathworld. *MathWorld—A Wolfram Web Resource*. [mathworld.wolfram.com](http://mathworld.wolfram.com).